JOURNAL OF THE AMERICAN WATER RESOURCES ASSOCIATION
FEBRUARY AMERICAN WATER RESOURCES ASSOCIATION 2006

EVALUATION OF NEXRAD STAGE III PRECIPITATION DATA OVER A SEMIARID REGION[1]

Hongjie Xie, Xiaobing Zhou, Jan M.H. Hendrickx, Enrique R. Vivoni, Huade Guan, Yong Q. Tian, and Eric E. Small[2]

ABSTRACT: This study examines NEXRAD Stage III product (hourly, cell size 4 km by 4 km) for its ability in estimating precipitation in central New Mexico, a semiarid area. A comparison between Stage III and a network of gauge precipitation estimates during 1995 to 2001 indicates that Stage III (1) overestimates the hourly conditional mean (CM) precipitation by 33 percent in the monsoon season and 55 percent in the nonmonsoon season; (2) overestimates the hourly CM precipitation for concurrent radar-gauge pairs (nonzero value) by 13 percent in the monsoon season and 6 percent in the nonmonsoon season; (3) overestimates the seasonal precipitation accumulation by 11 to 88 percent in monsoon season and underestimates by 18 to 89 percent in the nonmonsoon season; and (4) either overestimates annual precipitation accumulation up to 28.2 percent or underestimates it up to 11.9 percent. A truncation of 57 to 72 percent of the total rainfall hours is observed in the Stage III data in the nonmonsoon season, which may be the main cause for both the underestimation of the radar rainfall accumulation and the lower conditional probability of radar rainfall detection in the nonmonsoon season. The study results indicate that the truncation caused loss of small rainfall amounts (events) is not effectively corrected by the real-time rain gauge calibration that can adjust the rainfall rates but cannot recover the truncated small rainfall events. However, the truncation error in the monsoon season may be suppressed due to the larger rainfall rate and/or combined effect of overestimates by bright band and hail contaminations, virga, advection, etc. In general, improvement in NEXRAD performance since the monsoon season in 1998 is observed, which is consistent with the systematic improvement in the NEXRAD network.
(KEY TERMS: precipitation; NEXRAD; rain gauge; time series analysis; truncation error; statistics.)

Xie, Hongjie, Xiaobing Zhou, Jan M.H. Hendrickx, Enrique R. Vivoni, Huade Guan, Yong Q. Tian, and Eric E. Small, 2006. Evaluation of NEXRAD Stage III Precipitation Data Over a Semiarid Region. Journal of the American Water Resources Association (JAWRA) 42(1):237-256.

INTRODUCTION

Although weather radar has assisted meteorological precipitation predictions for over 40 years, its operational use in hydrologic applications spans only about a decade (Krajewski and Smith, 2002). The National Weather Service (NWS) began the installation of the NEXRAD system across the United States in 1991. The resulting 158 radars, known as WSR-88D (Weather Surveillance Radar-1988 Doppler), have revolutionized the NWS forecast and warning programs through improved detection of severe wind, rainfall, hail, and tornadoes. NEXRAD rainfall data products (e.g., Stages I, II, III, and IV) have been used to analyze the statistical characteristics of extreme rainfall and hydrometeorological events (Smith *et al.,* 2001, 2002; Zhang and Smith, 2003), validate satellite remote sensing algorithms (Krajewski and Smith, 2002; Habib and Krajewski, 2002), and perform flood predictions (Finnerty *et al.,* 1997; Vieux and Bedient, 1998; Bedient *et al.,* 2000). Furthermore, continuous and spatially distributed radar rainfall data are a critical input to climate, weather, and hydrologic models.

Despite considerable evaluation studies (Pereira Fo *et al.,* 1998, 1999a; Johnson *et al.,* 1999; Stellman *et al.,* 2000; Grassotti *et al.,* 2003; Morin *et al.,* 2003; Jayakrishnan *et al.,* 2004), the quality of multisensor NEXRAD rainfall products is still under investigation, in particular over complex terrain (Young *et al.,*

[1]Paper No. 04055 of the *Journal of the American Water Resources Association* (JAWRA) (Copyright © 2006). **Discussions are open until August 1, 2006.**

[2]Respectively, Assistant Professor, Department of Earth and Environmental Science (EES), University of Texas at San Antonio, 6900 North Loop 1604 West, San Antonio, Texas 78240; Assistant Professor, Department of Geophysical Engineering, Montana Tech of the University of Montana, 1300 West park Street, Butte, Montana 59701; Professor of Hydrology (Hendrickx), Assistant Professor of Hydrology (Vivoni), and Ph.D. Student of Hydrology, Department of EES, New Mexico Tech, Socorro, New Mexico 87801; Assistant Professor of GIS, Department of Earth and Geographic Science, University of Massachusetts, Boston, Massachusetts 02125-3393; and Assistant Professor of Geology, Department of Geological Science, University of Colorado, Boulder, Colorado 80309-0399 (E-Mail/Xie: hongjie.xie@utsa.edu).

1999) and in regions of poor radar coverage (Maddox *et al.,* 2002). One motivation for continued weather radar evaluations is the increasing use of radar rainfall products as inputs to hydrologic models (Pereira Fo *et al.,* 1999a,b; Jayakrishnan *et al.,* 2004; Bedient *et al.,* 2000). Since errors in radar estimation propagate to streamflow (e.g., Shah *et al.,* 1996; Winchell *et al.,* 1998), it is essential to understand the potential effects of rainfall errors on hydrologic predictions. Distributed hydrologic models in particular are sensitive to rainfall spatial distribution, intensity, and timing since the rainfall products used in these models are not averaged over the basin area. Gauge rainfall is still the only reference for ground truth, though the gauge rainfall itself has random, systematic, and representative or sampling errors (Habib *et al.,* 2001; Kitchen and Blackall, 1992; Ciach and Krajewski, 1999). A very common way to evaluate the radar rainfall (RR) estimation error is to evaluate the radar-gauge (R-G) difference using standard statistical methods such as the standard deviation, error variance, and mean bias (mean gauge rainfall/mean radar rainfall). Nevertheless, hydrometeorologists realize that the R-G difference cannot be treated as RR error because rain gauges do not measure spatially averaged rainfall accumulations on a spatial scale of a NEXRAD pixel (Zawadzki, 1975; Krajewski, 1987; Kitchen and Blackall, 1992; Ciach and Krajewski, 1999; Anagnostou *et al.,* 1999). Ciach and Krajewski (1999) derived an area point error variance method to partition the R-G difference variance into RR error variance and gauge sampling (representativeness) error variance. However, this method requires an estimation of the spatial correlation function over a radar pixel scale (Krajewski *et al.,* 2003). This function can be derived from a high density rain gauge cluster within a radar cell.

Unfortunately, a high density rain gauge cluster is not always available. The NWS still adjusts the radar estimate to match the gauge estimation by multiplying the mean bias to the radar estimates (Stage I), and then producing Stage II and Stage III products. The most commonly used NEXRAD product in hydrometeorological applications is the NEXRAD Stage III data (e.g., Young *et al.,* 2000), since it (1) involves the correction of radar rainfall rates with multiple surface rain gauges and has a significant degree of meteorological quality control by trained personnel at individual River Forecast Centers (RFCs) (Fulton *et al.,* 1998); (2) merges adjacent radar precipitations to reduce the effects of spatially variable biases in range direction from individual radars (Bradley *et al.,* 2002); (3) can estimate precipitation when gauge densities are low, in particular when there is convective precipitation, in which case the spatial variations in precipitation are large and not detectable by the sparse gauge network (Young *et al.,* 2000); and (4) covers an entire RFC, so basin wide hydrologic analyses are possible. Yet, it should be realized that Stage III also suffers errors from mosaicking of several radars as well as some errors inherited from Stage I and Stage II data such as Z-R (reflectivity – precipitation) relation, hail contamination, beam overshooting, brightband, range dependence, virga, and advection (Austin, 1987; Smith *et al.,* 1996; Pereira Fo *et al.,* 1998; Morin *et al.,* 2003).

Another NEXRAD product called P1, implemented at Arkansas-Red Basin River Forecast Center (ABRFC), utilizes a local bias adjustment algorithm. P1 first merges the Stage I hourly digital precipitation (HDP) product for the entire RFC, and then adjusts each cell in the merged HDP product by multiplying a local bias (gauge rainfall/radar rainfall). For a cell that does not have a collocated rain gauge, a distance weighting scheme is used to generate a bias (Young *et al.,* 2000; Seo and Breidenbach, 2002). In general practice at the ABRFC, the P1 product works well in gauge rich areas, particularly for widespread stratiform rainfalls in the cold season, and the Stage III product works well in warmer seasons (Seo and Breidenbach, 2002; NWS, 2002).

A major error that the NWS discovered in the NEXRAD Stage I product is a truncation error in processing NEXRAD rainfall rates (Seo *et al.*, 2000; McCollum *et al.,* 2002; Fulton *et al.,* 2003). A truncation error can also result from the sensitivity of the radar antenna, analog to digital conversion, etc. However, for the Stage III product, Fulton *et al.* (2003) suggested that the truncation impact is not likely to be large since the Stage III product has been calibrated by real-time gauge data. Yet, Pereira Fo *et al.* (1998) found a 40 percent underestimate of accumulative rainfall (Stage III) from June 1995 to July 1996 in the Oklahoma Mesonetwork. Young *et al.* (2000) noted that the Stage III product from ABRFC can result in significantly fewer precipitation hours in the case of light precipitation, and that the overall Stage III estimates were approximately 20 percent lower when compared with the gauge observations. Fortune (2002) found that Stage III products were approximately 25 percent lower in comparison with the 24-hour gauge observations. Jayakrishnan *et al.* (2004) found an overall underestimate of Stage III data from 1995 to 1999 over the Texas-Gulf basin. Despite these studies, there have yet to be quantitative evaluations on the radar truncation error impact on the Stage III rainfall product or on the differential impact of the truncation error on the hourly CM precipitation, hourly CM for concurrent radar gauge pairs (nonzero value), and seasonal precipitation accumulations in monsoonal and nonmonsoonal rainfall events.

This study evaluates the ability of the NEXRAD Stage III product in detecting precipitation in a semiarid area of central New Mexico with a focus on the seasonal variability of radar measurement during the monsoon and nonmonsoon seasons. Since the Stage III product does not incorporate the rain gauge data in the study area during the multisensor data fusion, radar gauge intercomparison in the study area seems to be the best way to evaluate the overall quality of the NEXRAD Stage III product. In this study, the NEXRAD rainfall estimates were found to behave very differently between the monsoon and nonmonsoon seasons in the study area. Another purpose of this study is to examine the possible error sources in the Stage III product through radar-gauge intercomparison. The results indicate that multiple error sources exist but the truncation error may still be a major one, especially during the nonmonsoon season (October through May).

STUDY AREA AND DATA SOURCES

The study area is the Sevilleta National Wildlife Refuge (NWR), about 920.6 km^2, located in central New Mexico (Figure 1). Elevation of the study area ranges from 1,400 m at the Rio Grande River, 1,550 to 1,700 m in most of the flat areas, and up to about 2,200 m at the Los Pinos Mountains in the northeastern part. The Sevilleta NWR is the primary research site of the Sevilleta Long-Term Ecological Research Program (LTER) (Hobbie *et al.,* 2003) and is also one of the National Aeronautical and Space Administration's BigFoot sites used to validate remote-sensing data products and algorithms. The Sevilleta NWR is a biome transition of grassland, shrubland, woodland, and riparian forests. Because of the confluence of these major biome zones, the Sevilleta NWR presents an ideal setting to investigate how climate variability and climate change act together to affect ecosystem dynamics (University of New Mexico Biology, 2003, unpublished LTER site review). In the study area, El Niño-Southern Oscillation events strongly influence nonmonsoon precipitation (Dahm and Moore, 1994), while no clear links have been found during the summer monsoon season (Moore, 1996). A study using the data from the Socorro weather station, 24 km south of the Sevilleta NWR, indicated that rainfall from October through May increased by 53 percent in El Niño years and decreased by slightly more than half in La Niña years when compared to the mean rainfall over the past 80 years of 237.6 mm (Dahm and Moore, 1994).

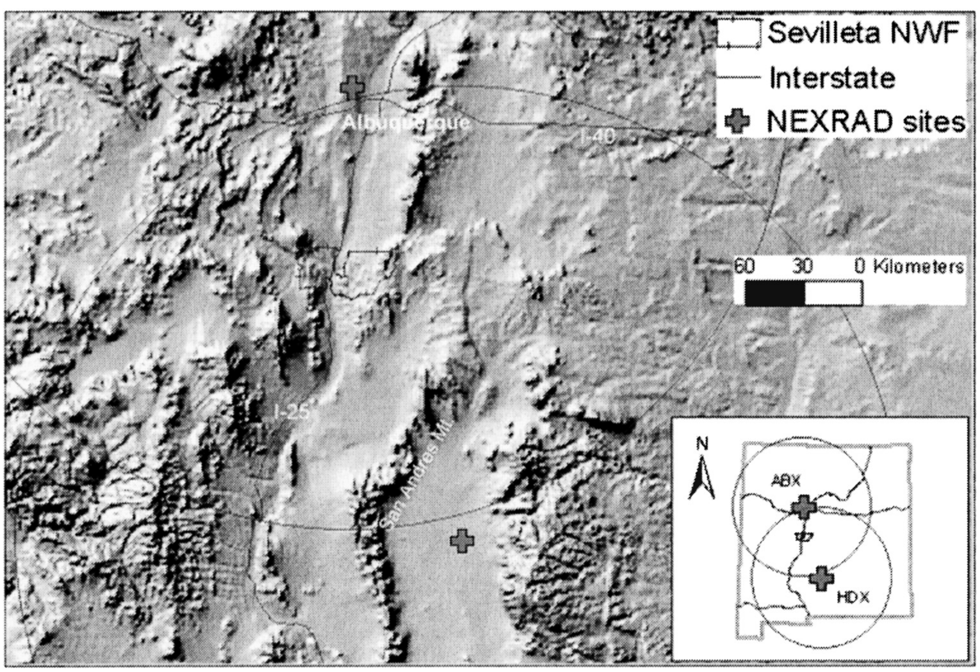

Figure 1. Index Map of the Study Area. The background image is a shaded relief DEM (NGDC, 2003).

Gauge Data

There are ten permanent meteorological stations within the Sevilleta NWR operated by the Sevilleta LTER program (Figure 2, Table 1). Seven of them (labeled 1 and 40 to 45) have continuous rainfall records since 1995, thus temporally overlapping the NEXRAD Stage III data. Instruments in each station continuously record precipitation, and record other climate variables, such as air temperature, relative humidity, wind speed and direction, and solar radiation, on an hourly basis. During rainfall periods, precipitation is recorded on a one-minute basis. All rain gauges are tipping bucket type fabricated by Langmuir Laboratory for Atmospheric Research at New Mexico Institute of Mining and Technology (New Mexico Tech) (1 tip = 0.25 mm) or manufactured by Texas Electronics (TE5Z5MM) (1 tip = 0.1 mm). However, most of the gauges are Texas Electronics gauges. After calibration, the minimum rain rate per hour for these gauges is 0.103 mm/h. A funnel collector next to each gauge is used to calibrate the gauge estimates. Radio and telephone links are used to download data on an eight-hour basis, with weekly site visits by the LTER meteorologists. Professional maintenance of these gauges on a regular basis keeps the random error at a minimum and thus improves the gauge data quality. For the period of 1989 to 2003, the mean annual precipitation within the study area was 253 mm, which is similar to the 80-year mean annual precipitation of 237.6 mm from the Socorro weather station. The hourly precipitation data in the period of 1995 to 2001 from the seven weather stations are used for the evaluation of NEXRAD Stage III estimates.

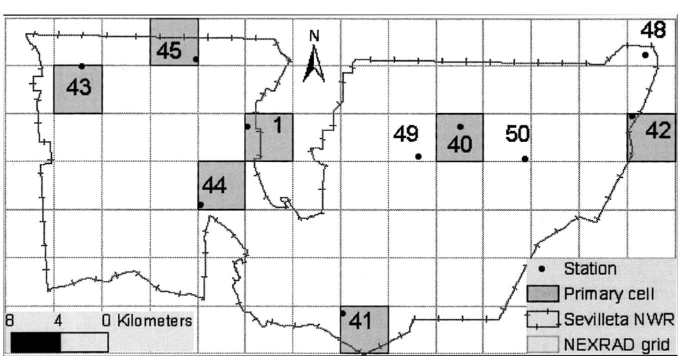

Figure 2. Location of Sevilleta NWR and Weather Stations Within the NWR With Coordinate System of UTM Zone 13 Projection and WGS 84 Datum. The primary cells and gauges indicated have been used for the comparisons in this study. Details about weather stations are in Table 1.

TABLE 1. Weather Station Information at the Sevilleta NWR (University of New Mexico, 2003).

Station ID	Name	Elevation (m)	Periods
1	Field Station	1,469	1991 to present
40	Deep Well	1,596	1987 to present
41	South Gate	1,538	1989 to present
42	Cerro Montoso	1,971	1989 to present
43	Red Tank	1,766	1989 to present
44	Rio Salado	1,503	1989 to present
45	Bronco Well	1,547	1990 to present
48	Savanna	1796	1,998 to present
49	Five Points	1,610	1999 to present
50	Blue Grama	1,669	2003 to present

Radar Data

The Sevilleta NWR is under the umbrella of two WSR-88D radars (Figure 1): Albuquerque (ABX) and Holloman Air Force Base (HDX) radars. The HDX radar station is at 1,286.87 m in elevation and about 130 to 170 km southeast of the Sevilleta NWR. The ABX radar station in Albuquerque is at 1,789.18 m in elevation and about 80 to 100 km north of the Sevilleta NWR. Vertical profiles (Figure 3) show the first four tilts (0.5, 1.5, 2.4, and 3.4 degrees) of the radar beam from the ABX and HDX radars to the Sevilleta NWR. There is no mountain blockage from the ABX radar to the study area, while the lowest radar elevation angle (0.5 degrees) from the HDX radar is blocked by the San Andres Mountains (a nearly north to south extension). The lowest beam altitude by the ABX radar tilt of 0.5 degrees is approximately 1.0 km on average above the Sevilleta NWR ground level. The lowest altitude by the HDX radar (1.5 degree tilt) is about 3.6 km on average above the Sevilleta NWR ground level, which may result in precipitation estimates with some uncertainties caused by advection, vertical profile changes, evaporation, and hail contamination (Morin *et al.,* 2003). In the NEXRAD precipitation products, data from the lowest of the four radar tilts with no significant beam blockage is typically used (Morin *et al.,* 2003). Thus, the 0.5 degree tilt of the ABX radar and 1.5 degree tilt of the HDX radar should be used to construct their corresponding precipitation products for the Sevilleta area. Short and Nakamura (2000) suggested that the mean storm heights over land are mostly in the range of 4 to 6 km and rarely less than 1 km. From the above analysis, overshooting from the ABX radar should not be a problem. The ABX radar should give very good rainfall estimates over the study area. Because the HDX radar is 130 to 170 km away from the Sevilleta area and the lowest beam height over the Sevilleta area is 3.6 km, the HDX radar should also give fairly good rainfall estimates, with possible underestimates caused by beam overshooting if the storm height is less than 3.6 km or overestimates when contaminated by advection, bright band, evaporation, and hail. The Stage III is a mosaicked Stage II product created by averaging nonzero rainfall accumulations, regardless of their distance from a radar site (Pereira Fo *et al.*, 1998). In this case, averaging the HDX radar rainfall with ABX radar rainfall might impact the mosaicked rainfall amount (reducing the accuracy of rainfall estimates), but it will not impact the total rainfall hours since averaging does not dismiss the rainfall hours. For example, if the ABX radar records rainfall in a particular hour while the HDX does not, that particular hour will still be stamped as a rainfall hour after averaging of rainfall amounts. So radar beam overshooting due to the HDX radar's 1.5 degree beam for the mosaicked Stage III product for the study area might result in a certain degree of uncertainty in terms of rainfall amount, but not in the total rainfall hours.

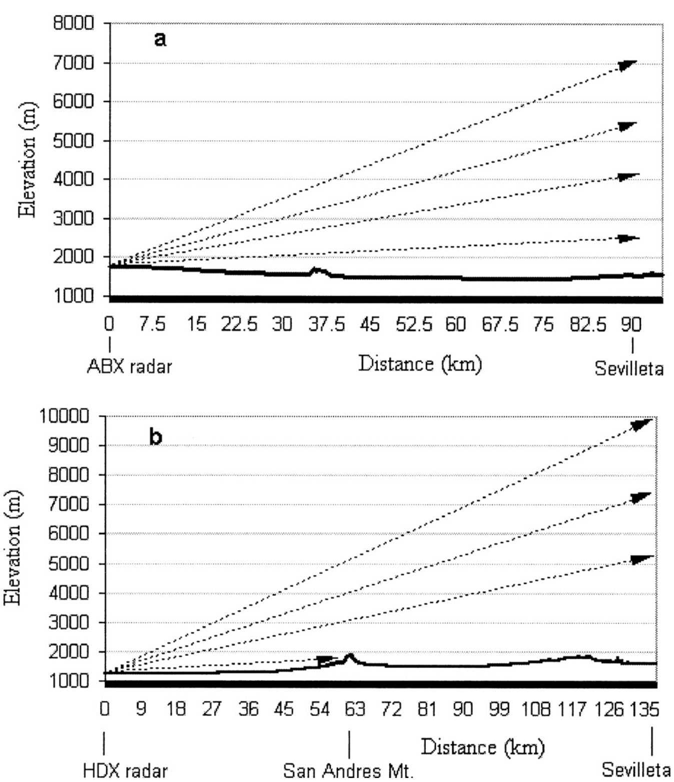

Figure 3. Vertical Profiles (dashed lines) showing the first four tilts (0.5, 1.5, 2.4, and 3.4 degrees) of radar beam from (a) ABX radar and (b) HDX radar to the Sevilleta NWR. The solid line denotes the ground surface elevation.

The NEXRAD Stage III precipitation data of the West Gulf River Forecasting Center (WGRFC) during 1995 to 2001 were downloaded from the National Weather Service (NWS, 2003). The original data set is in Hydrologic Rainfall Analysis Project (HRAP) projection or secant polar stereographic projection (Reed and Maidment, 1995, 1999) in multitarred and compressed binary formats. These data were transferred to a geographic information system (GIS) grid format, and the polar stereographic projection was defined using ArcGIS (Ormsby *et al.,* 2001, and then reprojected into Universal Transverse Mercator (UTM) projection, Zone 13 north, on the World Geodetic System 1984 (WGS84) datum. More details about Stage III projections and transformations are presented in Reed and Maidment (1995, 1999). These data are stored in a GIS-based database at New Mexico Tech (Xie *et al.,* 2003, 2005). Using the automatic data transformation and retrieval approaches developed by Xie *et al.* (2005), the precipitation data from 1995 to 2001 for the cells where Stations 1 and 40 to 45 are located (Figure 2) were retrieved. The Universal Time Coordinated (UTC) time of NEXRAD data were then transferred to U.S. Mountain Standard Time (MST) used at the Sevilleta NWR weather stations. The retrieved radar rainfall was then compared with the collocated rain gauge rainfall. For comparison purposes, the gauge records for precipitation corresponding to those records missing in the NEXRAD datasets were removed. The missing records were serious radar data gaps including the full months of August through November 2000 and December 2001, and most of July 2001 (Table 2).

METHODS

The statistical analyses are based on two seasons of a water year: nonmonsoon precipitation (October 1 through May 31) and monsoon precipitation (June 1 through September 30). To examine the probability distribution of radar and gauge rain rates in the study area, the rainfall count (hours), cumulative distribution frequency of rainfall count, and cumulative distribution frequency of rainfall amount during 1995 to 2001 for both radar and gauges were calculated. To quantify the differences between the radar and gauge estimates in the two seasons necessitated first examining some basic statistical characteristics such as precipitation accumulation, CM precipitation, hourly precipitation count, maximum precipitation, conditional variance of precipitation, and conditional coefficient of variation (CV). The conditional probability of rain detection (CPOD) for hourly precipitation measurements of 1995 to 2001 was then examined.

TABLE 2. Original NEXRAD Stage III Data From WGRFC (NWS, 2003).

Year	Jan	Feb	Mar	Apr	May	Jun	Jul	Aug	Sep	Oct	Nov	Dec
1995												
1996												
1997												
1998												2
1999	6	2										
2000								M	M	M	M	5
2001	13	7		2			22		1			M

Notes: Blank: Entire month available.
M: Entire month missing.
Number: Number of days missing.

Finally, a comparison was made of the concurrent gauge and radar estimates during the period 1998 to 2001 at various temporal scales (1 hour, 2 hours, 3 hours, 4 hours, 1 day, 15 days, 30 days, 60 days, and event based) for the CPODs, correlation coefficient (CC), and CM precipitation. Listed below are the definitions of some statistical approaches mentioned above.

Precipitation accumulation is the total precipitation in a particular time period. For example, the monsoonal precipitation accumulation is the sum of all rainfall amounts within the monsoon season.

Conditional mean (*CM*) precipitation is the average of precipitation accumulation over nonzero rainfall hours (Smith *et al.,* 1996), that is

$$\text{CM} = \text{precipitation accumulation/count of precipitation hours} \quad (1)$$

where CM and precipitation accumulation are in mm.

The CM differs from the mean precipitation, which is the average of precipitation accumulation over all hours (including no rainfall) in this period. The CM represents the average rainfall accumulation over nonzero rainfall hours during this period.

Radar CPOD (P_{rg}) is the probability (P) that radar can detect a rainfall that a collocated rain gauge (within the same cell) detects (McCollum *et al.,* 2002), that is

$$P_{rg} = P(R_r > 0 \mid R_g > 0) = radar\ \&\ gauge\_count / gauge\_count \quad (2)$$

where R_r (mm/h) is the radar measured precipitation rate, R_g (mm/h) is the gauge measured precipitation rate, *radar & gauge_count* is the hours of precipitation being concurrently detected by both the radar cell and the collocated gauge, and *gauge_count* is the total hours that the gauge detects precipitation.

Gauge CPOD (P_{gr}) is the probability (P) that a gauge can detect a rainfall that the collocated radar cell detects, that is

$$P_{gr} = P(R_g > 0 \mid R_r > 0 = gauge\ \&\ radar\_count / radar\_count \quad (3)$$

where *gauge & radar_count* is the same as above, and *radar_count* is the total hours that the collocated radar cell detects precipitation. The CPODs indicate the relative probability of rain detection for collocated pairs of radar cell and gauge in a period of time.

The correlation coefficient (CC) is the correlation of the radar rainfall intensity with the gauge rainfall intensity when a collocated radar cell and a gauge record the same rainfall event (nonzero rainfall value). The CC is defined as

$$CC = \frac{COV(R_r, R_g)}{\sigma(R_r)\sigma(R_g)} \quad (4)$$

where $COV(R_r,R_g)$ is the covariance of the collocated radar precipitation amounts and the gauge precipitation amounts (both are nonzero), $\sigma(R_r)$ is the conditional standard deviation of those collocated radar precipitation amounts (nonzero) and $\sigma(R_g)$ is the conditional standard deviation of those collocated gauge precipitation amounts (nonzero). The CC represents the correlation between the collocated radar estimates and gauge estimates when both see the same rainfall event at the same time. The larger the CC value, the better the relationship between the radar estimates and gauge estimates.

Conditional coefficient of variation (*CV*) measures the relative scattering in data with respect to the mean. It is defined as the conditional standard deviation of radar precipitation ($\sigma(R_r)$) or gauge precipitation ($\sigma(R_g)$) divided by the corresponding radar or gauge CM precipitation , that is

$$CV(r) = \frac{\sigma(R_r)}{radar\_CM} \tag{5}$$

$$CV(g) = \frac{\sigma(R_g)}{gauge\_CM} \tag{6}$$

where radar CM precipitation *radar_CM* and gauge CM precipitation *gauge_CM* are defined according to Equation (1). Both $\sigma(R_r)$ and $\sigma(R_g)$ are the same as in Equation (4).

RESULTS AND ANALYSIS

Probability Distribution of Radar and Gauge Rain Rates

Figures 4 and 5 illustrate the probability distribution of gauge and radar rainfall rates (intensities) in the monsoon seasons and nonmonsoon seasons of 1995 to 2001, respectively. The following are summaries of some important features from these figures.

Lower rainfall rates account for a larger portion of the total rainfall hours, but only a smaller portion of the total rainfall accumulation. For example, 50 percent of the rainfall hours with rainfall intensities less than or equal to 0.59 mm/h in the non-monsoon season or less than or equal to 0.87 mm/h (gauge) and 1.08 mm/h (radar) in the monsoon season contributes only 10 to 15 percent of the total rainfall accumulation (Table 3), and 10 percent of rainfall hours with rainfall intensities larger than 2.31 mm/h (gauge) or 3.42 mm/h (radar) in the nonmonsoon season and 4.91 mm/h (gauge) or 6.99 mm/h (radar) in the monsoon season contributes about 50 percent of total rainfall accumulation (Table 3). This suggests that high intensity rainfall events account for only a small portion of total rainfall hours but play an important role in the total rainfall amounts in this area.

The study area is characterized by lighter or stratiform precipitation in the nonmonsoon season, and heavier or convective precipitation in the monsoon season. From Table 3, the gauge estimates seem reasonable in the nonmonsoon season in which the rainfall rate is greater than or equal to 10 mm/h (or 20 mm/h) and only accounts for 0.2 percent (or 0.0

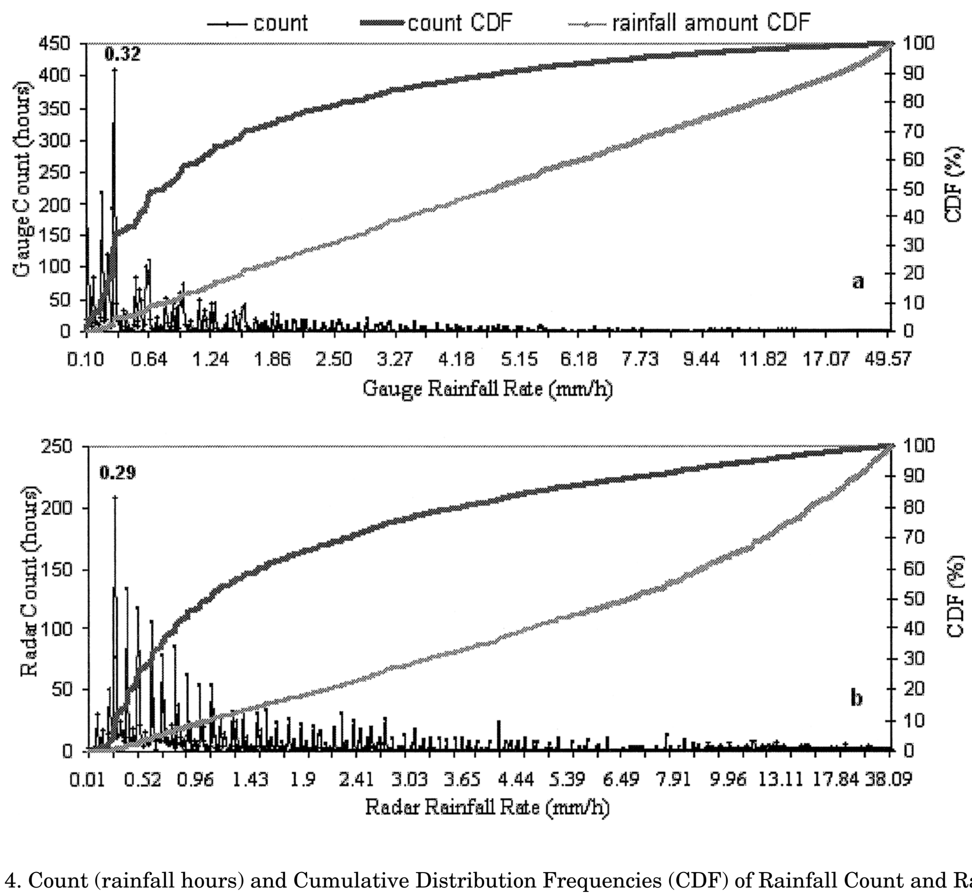

Figure 4. Count (rainfall hours) and Cumulative Distribution Frequencies (CDF) of Rainfall Count and Rainfall Amount at different (a) gauge and (b) radar rainfall rates in the monsoon seasons. Minimum rainfall rate calibrated is 0.103 mm/h for gauge and 0.01 mm/h for radar. Data are from the seven pairs of collocated radar cell and gauge during the period of 1995 to 2001, Sevilleta NWR, NM.

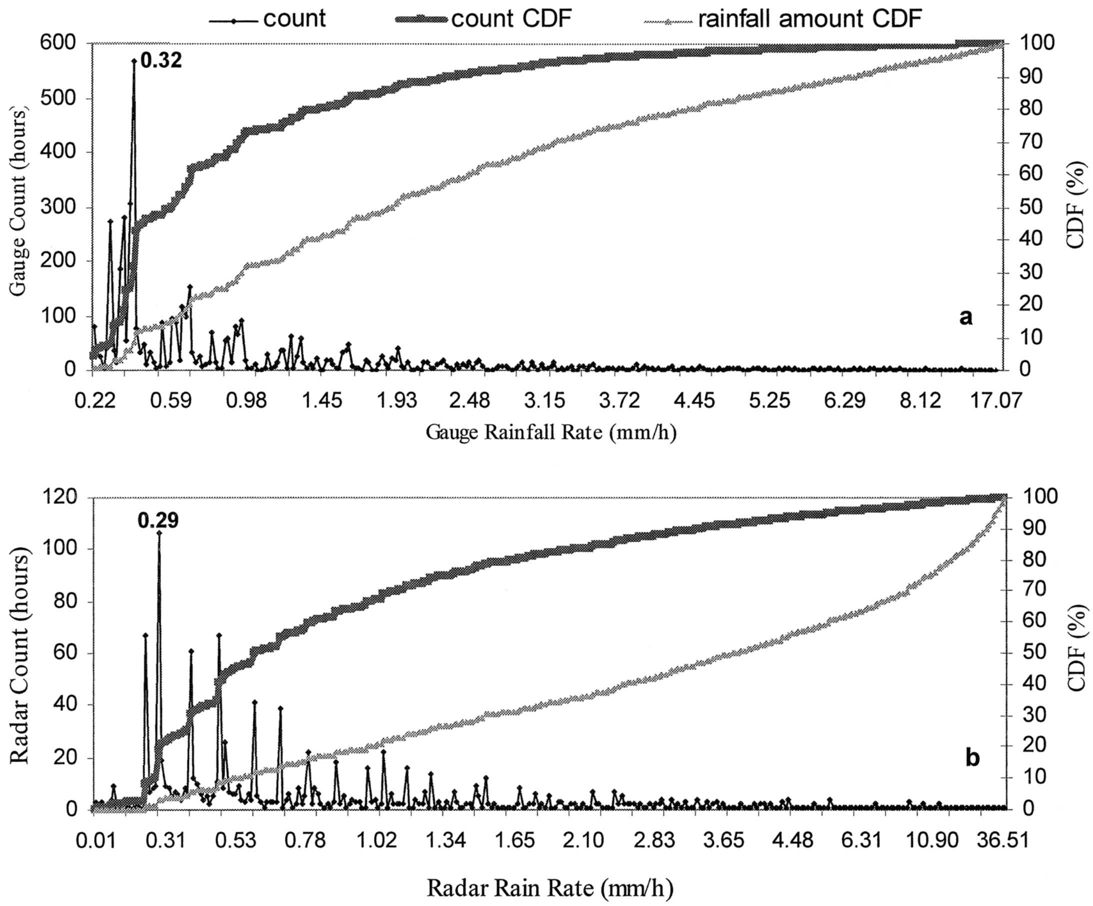

Figure 5. Count (rainfall hours) and Cumulative Distribution Frequencies of Rainfall Count and Rainfall Amount at Different (a) Gauge and (b) Radar Rainfall Rates in the Nonmonsoon Seasons.

TABLE 3. Probabilities of Radar and Gauge Rainfall Intensities (1995 to 2001) in Sevilleta.

				Monsoon					
Gauge	Rate[a] (mm/h)	≤0.32[d]	≤ 0.87	≤ 1.18	≤ 1.63	≤ 2.71	≤ 4.91	≥ 10	≥ 20
	CDFC[b] (percent)	32.8	50	60	70	80	90	2.8	0.6
	CDFA[c] (percent)	4.6	9.8	14.7	21.8	32.8	51.4	24.1	9.0
Radar	Rate[a] (mm/h)	≤ 0.29	≤ 1.08	≤ 1.53	≤ 2.28	≤ 3.59	≤ 6.99	≥ 10	≥ 20
	CDFC[b] (percent)	9.9	50	60	70	80	90	5.9	1.1
	CDFA[c] (percent)	0.9	10.1	15.1	22.1	32.7	51.2	36.1	11.1
				Nonmonsoon					
Gauge	Rate[a] (mm/h)	≤ 0.32	≤ 0.59	≤ 0.64	≤ 0.97	≤ 1.5	≤ 2.31	≥ 10	≥ 20
	CDFC[b] (percent)	42.7	50	60	70	80	90	0.2	0.0
	CDFA[c] (percent)	11.8	14.9	21.9	29.9	41.5	58.9	2.8	0.5
Radar	Rate[a] (mm/h)	≤ 0.29	≤ 0.59	≤ 0.81	≤ 1.14	≤ 1.66	≤ 3.42	≥ 10	≥ 20
	CDFC[b] (percent)	19.1	50	60	70	80	90	2.5	0.7
	CDFA[c] (percent)	3.1	12.1	16.7	22.7	31.2	46.9	27.7	13.6

[a]Rainfall rate.
[b]Cumulative distribution frequency of rainfall counts or hours (CDFC).
[c]Cumulative distribution frequency of rainfall amount (CDFA).
[d]The rainfall rate with largest probability of rainfall occurrence (see Figures 4 and 5).

percent) of the total rainfall hours, contributing only 2.8 percent (or 0.5 percent) of total rainfall accumulation. However, from the radar records in the same period, the rainfall rate greater than or equal to 10 mm/h (or 20 mm/h) accounts for 2.5 percent (or 0.7 percent) of the total hours, a little bit larger than the gauge's, but contributing 27.7 percent (or 13.6 percent) of the total rainfall amount. This suggests that in the nonmonsoon season, radar either overestimates rainfall rates for large rainfall events, or misses small rainfall events (such as truncation error — please see later discussion), or both. Yet in the monsoon season, radar and gauge estimates for rainfall rates greater than or equal to 10 mm/h (or 20 mm/h) seem fairly similar in terms of contributions to rainfall hours and rainfall amounts, although the radar contributions are a little bit larger than those of gauges. This suggests that in the monsoon season the radar and gauge estimates are reasonably matched with a certain degree of radar overestimation at large rainfall rates.

The gauge rainfall intensity of 0.32 mm/h and radar rainfall intensity of 0.29 mm/h (see Figures 4 and 5) have the largest probabilities of rainfall occurrence: 9.1 percent (monsoon) and 11.5 percent (nonmonsoon) for gauge, and 5 percent (monsoon) and 8.8 percent (nonmonsoon) for radar. These probabilities contribute 1.5 percent (monsoon) and 3.6 percent (non-monsoon) of total rainfall hours for gauge, and 0.6 percent (monsoon) and 1.6 percent (nonmonsoon) for radar (not shown in Figures 4 and 5).

At rainfall intensities less than or equal to 0.32 mm/h, gauges record 32.8 percent (monsoon) and 42.7 percent (nonmonsoon) of total rainfall hours, accounting for 4.6 percent and 11.8 percent of total rainfall accumulation in the monsoon and non-monsoon seasons, respectively, while radar records 12.0 percent and 22.0 percent of total rainfall hours, accounting for 0.9 percent and 3.1 percent of total rainfall accumulation in the monsoon and nonmonsoon seasons, respectively. These results, together with those above, suggest that the gauge records larger percentages of rainfall hours and rainfall amounts at small rainfall rates than radar, while radar records larger percentages of rainfall hours and rainfall amounts at large rainfall rates than gauge. This phenomenon can be clearly seen in Figures 4(b) and 5(b), where the radar curves of the cumulative distribution frequency of rainfall amounts dip downward with a concave shape, and in Figures 4(a) and 5(a) where the gauge curves move upward with nearly a straight line shape.

Basic Statistical Characteristics

Figure 6 shows the time series of monthly rainfall accumulation (Figure 6a) and monthly rainfall hours (Figure 6b) for both the radar (seven cells) and the gauges (seven gauges) from 1995 to 2001. The temporal patterns of radar and gauge estimates show that the radar accumulation is larger than the gauge accumulation in the monsoon season and less than the gauge accumulation in the nonmonsoon season. The seasonal accumulation estimated by the radar during the nonmonsoon season is between 6.2 to 76.6 mm, while that estimated by the collocated gauges is between 16.3 to 133 mm (Table 4). However, during the monsoon seasons, the accumulation estimated by the radar is between 136.2 and 297.8 mm, while that estimated by the collocated gauges is between 91.5 and 268.2 mm (Table 4). The counts of precipitation hours have almost the same patterns as the accumulation except for June and September in the monsoon season of 1997 when the radar observed fewer hours than the gauges. As shown in Figure 7, the difference of the annual rainfall accumulation between the radar and the gauges decreases with increase of time (year). Figure 7 also illustrates that the total annual counts of precipitation hours recorded from the radar are 18 to 43 percent less than those from the gauges, mainly because of the much fewer counts of rainfall hours recorded by the radar in the nonmonsoon seasons. These results are also shown in Table 4, in which the annual biases range from 0.78 to 1.14, corresponding to 28.2 percent overestimates to 11.9 percent underestimates, respectively. Table 4 also shows the seasonal biases: 0.53 to 0.90 in the monsoon seasons and 1.22 to 9.45 in the nonmonsoon seasons, implying a radar overestimation by 11 to 88 percent in the monsoon season and an underestimation by 18 to 89 percent in the nonmonsoon season.

Figure 8 shows the maximum hourly precipitation rate (Figure 8a) and seasonally CM precipitation rate and conditional variance of hourly precipitation (Figure 8b) for both the radar and the gauges. The hourly maximum precipitation rates from both the gauges and radar show a similar pattern: they are larger in the monsoon season than in the nonmonsoon season. This is because of the heavier rainfalls of convective thunderstorms in the monsoon seasons and lighter stratiform type precipitation in the nonmonsoon seasons. There are exceptions in 1997 and 2000 when the radar maximum precipitation in the nonmonsoon season is larger or close to that in the monsoon season. The maximum precipitation rate in the nonmonsoon season is 36.53 mm/h observed on May 21, 1997, ending at 15:00 MST, and it is 39.03 mm/h observed on April 28, 2000, ending at 15:00 MST. These exceptions may suggest that the monsoon seasons in these two years came earlier, or radar overestimated the precipitation due to various reasons such as hail and/or bright band contamination.

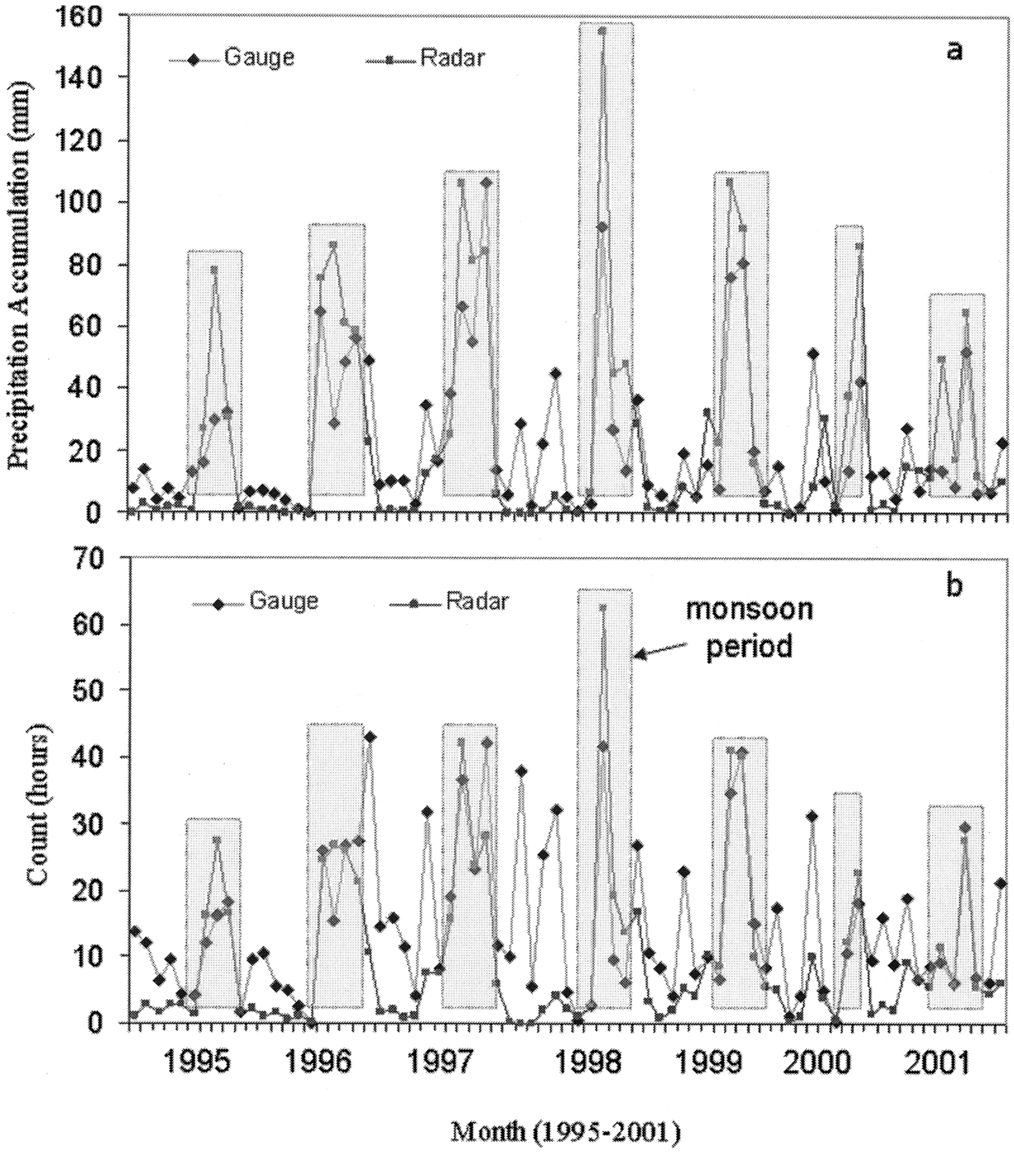

Figure 6. Time Series of Monthly (a) Rainfall Accumulation and (b) Rainfall Hours for Both the Radar and the Gauges. Shaded areas are in monsoon seasons. Some radar data are missing in 2000 and 2001 (see Table 2).

The CM precipitation has the same seasonal variability: both radar and gauge CMs in the monsoon season are always larger than those in the nonmonsoon season, and the radar CMs are always larger than the gauge CMs. The radar CMs are between 2.21 to 2.85 mm/h and 0.78 to 1.82 mm/h in the monsoon seasons and nonmonsoon seasons, respectively. The gauge CMs are between 1.54 to 2.21 and 0.75 to 1.29 in the monsoon seasons and nonmonsoon seasons, respectively.

Similar to the maximum precipitation and CM precipitation, the conditional variance of precipitation is larger in the monsoon season than in the nonmonsoon season. The conditional variances of gauge estimates are between 5.9 and 15.3 $(mm/h)^2$ in the monsoon seasons and 1.2 to 3.3 $(mm/h)^2$ in the nonmonsoon seasons. The conditional variances of radar estimates are between 11 and 18.2 $(mm/h)^2$ in the monsoon seasons and 0.4 and 7.5 $(mm/h)^2$ in the nonmonsoon seasons. Generally, the conditional variance in monsoon seasons is larger than that in nonmonsoon seasons. Two exceptions for this are the larger variances [13.2 and 28.7 $(mm/h)^2$] from radar estimates in nonmonsoon than monsoon season observed in 1997 and 2000 due to the two larger maximum rainfall rates mentioned above.

To further study the relative scattering in radar and gauge estimates, the CVs are calculated. By excluding the above two larger precipitation rates from calculation, the mean CVs of radar and gauge in

TABLE 4. Precipitation Accumulation and Bias From Seven Pairs of Collocated Radar Cell and Gauge (1995 to 2001).

Water Year	Gauge[a] (mm)	Radar[b] (mm)	Bias[c]	Period	Gauge[a] (mm)	Radar[b] (mm)	Bias[c]
1995				M	91.5	136.2	0.67
1996	224.6	287.9	0.78	NM	26.3	6.2	4.24
				M	198.3	281.7	0.70
1997	401.2	353.3	1.14	NM	133	55.5	2.40
				M	268.2	297.8	0.90
1998	260	269.6	0.96	NM	123.8	13.1	9.45
				M	136.2	256.5	0.53
1999	278	314.5	0.88	NM	93.7	76.6	1.22
				M	184.3	237.9	0.77
2000	192.6			NM	87.6	47.4	1.85
				M	105		
2001	290.3			NM	179.2		
				M	111.1		

[a]Gauge precipitation accumulation.
[b]Radar precipitation accumulation.
[c]Bias: Gauge precipitation accumulation/radar precipitation accumulation. A bias less than 1 indicates that the radar overestimated, and larger than 1 indicates that the radar underestimated, the rainfall collected at the rain gauges.
M: Monsoon season (June to September).
MM: Nonmonsoon season (October to May).

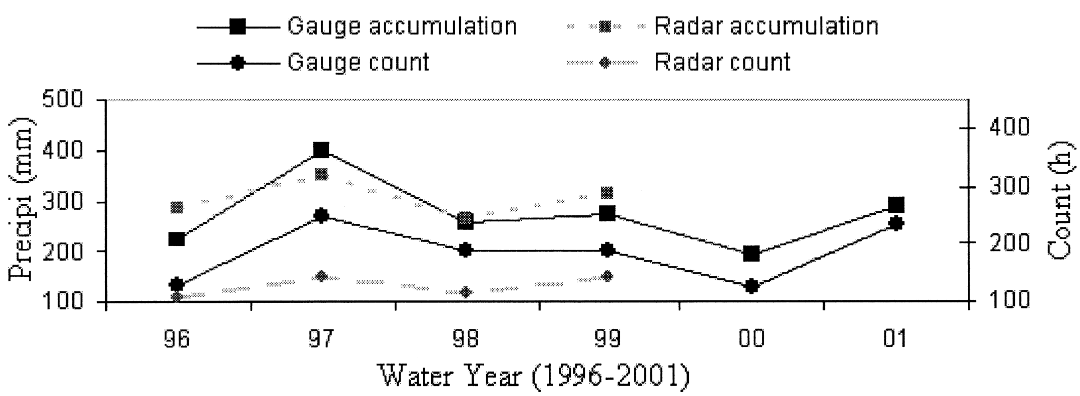

Figure 7. Time Series of Annual Precipitation Accumulation and Precipitation Hours (count) From Both the Radar and the Gauges. There are only four completed water years of data due to lack of nonmonsoon data for the 1995 water year, and some radar data are missing for 2000 and 2001 water years (Table 2).

the nonmonsoon seasons of the seven years (1995 to 2001) are 1.20 and 1.25, respectively, while in the monsoon seasons they are 1.58 and 1.62, respectively. The radar CV is smaller than the gauge CV, suggesting that even though the radar has a larger conditional variance than the collocated gauge, the point gauge estimates are more scattered than the areal radar estimates — just as expected.

Conditional Probability of Rainfall Detection (CPOD) in Sevilleta NWR

Figure 9 shows the time series of CPOD in the Sevilleta NWR. The radar CPOD is much lower than the gauge CPOD ($P_{rg} < P_{gr}$) in the nonmonsoon seasons, while it is slightly higher than the gauge CPOD ($P_{rg} < P_{gr}$) in monsoon seasons (except for the monsoon seasons of 1997 and 2001). This corroborates

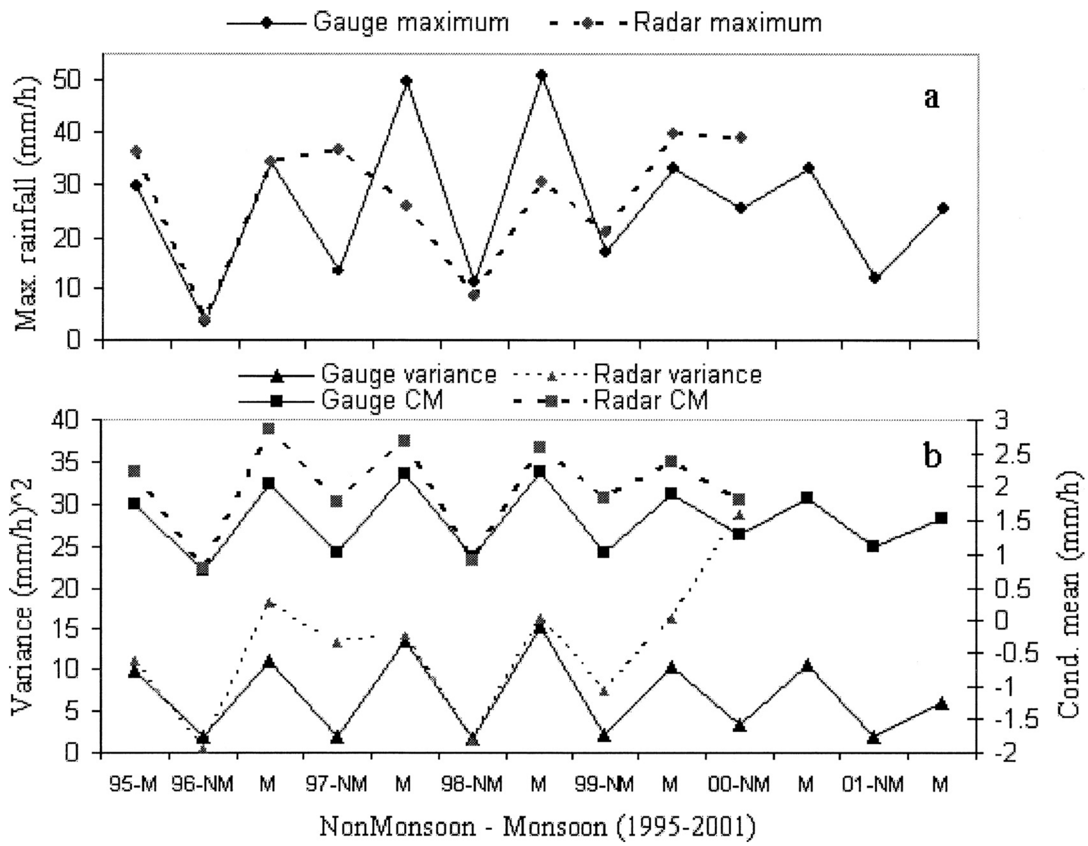

Figure 8. Time Series of (a) Seasonal Maximum Precipitation Rate and (b) Conditional Mean (CM) Precipitation Rate and Conditional Variance of Precipitation for Both the Radar and the Gauges. Some radar data are missing in 2000 and 2001 (see Table 2) (M: monsoon season, NM: nonmonsoon season).

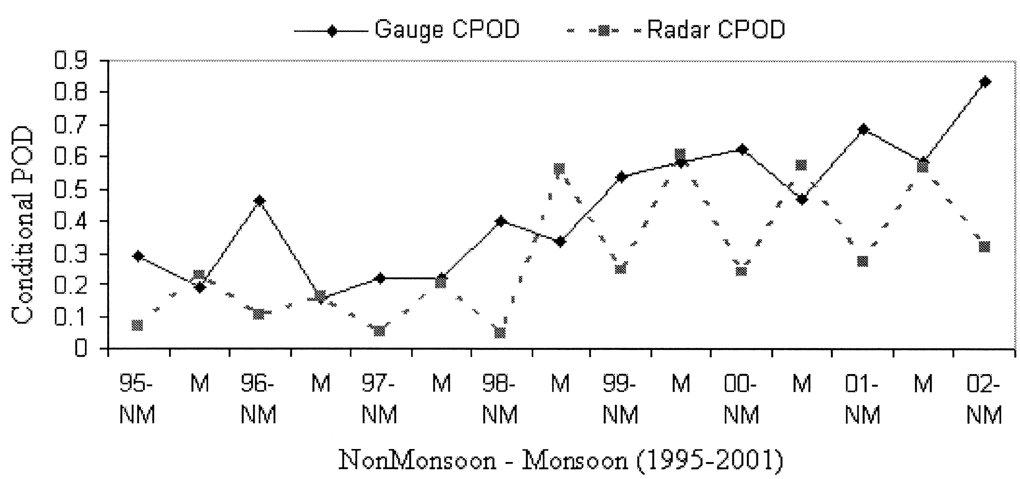

Figure 9. Time Series of the Conditional Probability of Rainfall Detection (CPOD) for Gauges and Radar. The "02-NM" only includes data from October to November 2001; the "95-NM" only includes data from January to May 1995 (M: monsoon season, NM: nonmonsoon season).

what McCollum *et al.* (2002) found from the collocated 24-hour accumulation of NEXRAD HDP product and gauges in the continental United States for a time period of three years (1998 to 2001). Furthermore, the radar CPOD is larger in the monsoon than the nonmonsoon season (Figure 9), which suggests that the radar either detects rainfall better in the monsoon season than the nonmonsoon season, or underestimates rainfall in the nonmonsoon season, or both. The larger gauge CPOD in the nonmonsoon than the monsoon season suggests that the gauges have a better capability to detect stratiform rainfalls in the nonmonsoon season than to detect convective rainfalls in the monsoon season. The overall increase of the radar and gauge CPODs with time starting from the monsoon season of 1998 may indicate that the estimation of NEXRAD precipitation has increasingly been improved since then. By far one of the most difficult problems with the Stage III data has been the systematic biases, particularly before mid-1997 (NWS, 2002). Many of the recent efforts have been made primarily to reduce the systematic biases (NWS, 2002; Johnson *et al.,* 1999; Stellman *et al.,* 2000; Wang *et al.,* 2000) by reducing the mean error and conditional mean error at a basin scale. The results indicate that in the West Gulf RFC, significant improvements have been made since the monsoon season of 1998. Jayakrishnan *et al.* (2004) found similar improvement since 1998, but their analysis did not separate the monsoon season from the nonmonsoon season, while the results contained herein clearly indicate the improvement since the monsoon season of 1998.

Comparison of Concurrent Gauge and Radar Estimates at Various Temporal Scales

Table 5 shows the statistics of precipitation estimates from the collocated seven radar cells and seven gauges during the period of 1995 to 2001. There are 606 pairs of radar gauge with nonzero rainfall value in the nonmonsoon seasons and 1,330 pairs in the monsoon seasons. The precipitation observed by the radar against that observed concurrently by the gauges for the monsoon and nonmonsoon seasons is plotted in Figure 10. The difference is as high as 32.4 mm/h in the nonmonsoon seasons and 41.8 mm/h in the monsoon seasons. The CC (Equation 4) of rainfall amounts between radar gauge data pairs is 0.406 for the nonmonsoon seasons and 0.183 for the monsoon seasons (Figure 10). These CCs confirm the positive covariation between the radar and gauge estimates as expected. However, only 16.0 percent (squared correlation) of variance on the radar and gauge estimates is in common for the nonmonsoon seasons and 3.0 percent for the monsoon seasons.

TABLE 5. Statistics of Radar and Gauge Estimations in the Monsoon and Nonmonsoon Season (1995 to 2001).

Statistical Items	Nonmonsoon	Monsoon
Total Hours of Precipitation		
Radar	1,143	3,900
Gauge	4,181	3,540
Total Hours of Radar Gauge Pairs With Nonzero Values	606	1,330
Conditional Probability of Rain Detection (percent)		
Gauge	0.53	0.34
Radar	0.14	0.38
Correlation Coefficient of Precipitation in Pairs (percent)	0.41	0.18
Conditional Mean Precipitation (mm)		
Radar	1.60	2.65
Gauge	1.03	1.74
Conditional Mean Precipitation in Pairs (mm)		
Radar	1.84	3.07
Gauge	1.74	2.72

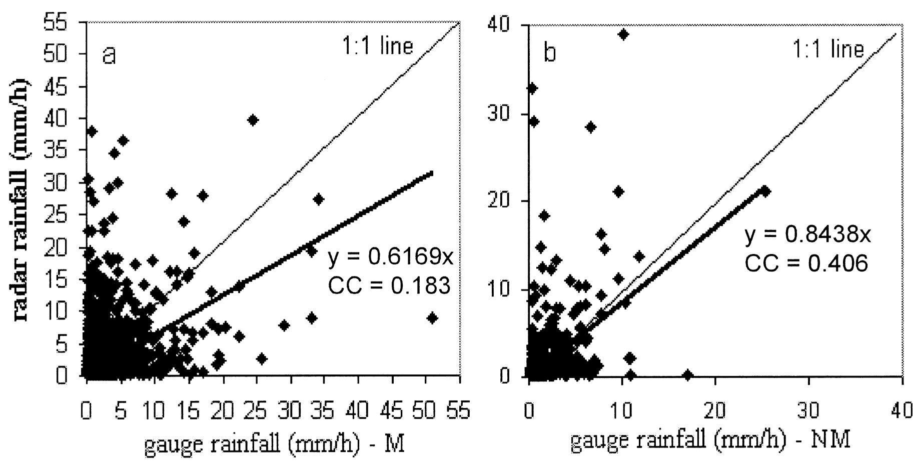

Figure 10. Scatter Plot of Hourly Rainfall of (a) 1,331 Pairs of Radar-Gauge Data in the Monsoon (M) Season and (b) 606 Pairs in the Nonmonsoon (NM) Season.

To further investigate the difference between the concurrent radar and gauge estimations (nonzero) at the Sevilleta NWR, CPOD, CC, and CM have been analyzed at different temporal scales (1 hour, 2 hours, 3 hours, 4 hours, 1 day, 15 days, 30 days, 60 days, and event based). The previous CPOD analysis suggests that the radar estimation has been improved since the monsoon season of 1998, so the data used here are only from the monsoon seasons of 1998 to 2001.

Figure 11 shows that both the radar and gauge CPODs increase as the temporal scale increases. The CPODs are up to 0.9 in the 15-day accumulation and nearly 1.0 in the 30-day accumulation. The gauge CPODs in the nonmonsoon seasons and the radar CPODs in the monsoon seasons have the largest values and almost the same trend of change, while the radar CPODs in the nonmonsoon seasons have the smallest values. The gauge CPODs in the monsoon seasons have medium values.

Unlike the behavior of CPODs at the temporal scale, the CCs of radar-gauge pairs change in a totally different way (Figure 11). The overall CCs for both monsoon and nonmonsoon seasons start from gradually decreasing, to increasing, and then decreasing again with the increasing temporal scale. The differences of the CCs between nonmonsoon season and monsoon season are mainly due to the behaviors of radar rainfall estimates during these two seasons. Table 6 shows that the concurrent radar CM (2.52 mm) in the nonmonsoon season starts to be less than the concurrent gauge CM (2.66 mm) when the temporal scale increases to three hours. This is because, as the time scale increases and sample size decreases, the gauge has more hours of precipitation measurement (1,802 hours total) to be added to the accumulation than the radar has (only 746 hours total). In the nonmonsoon season, the hourly rainfall has the largest CC (approximately 0.48) between radar and gauge. In the monsoon season, however, the radar CMs are always larger than the gauge CMs since the radar has more rainfall hours to be added than the gauge as the time scale increases. The CC decreases first, then increases to 0.73 (30-day scale), and then decreases to 0.44 (60-day scale), which is close to the value at the 1-day scale (0.42). It is expected that CCs will increase as the time scale increases (Habib and Krajewski, 2002). However, Figure 11 shows that at the 60-day scale, the CC decreases. The cause for this is not clear but increasing time scale and subsequent decreasing sampling size will affect the CC value. At some time scale (for instance, 60-day), the sampling size may not be large enough to guarantee the correct CC calculation.

An event based accumulation analysis (not shown) was conducted by adding all continuous hourly precipitation measurements together as an independent rainfall event. It was found that the CCs for a rainfall event are the same as those of a four-hour accumulation, while other statistical parameters are close to 1 hour, 2 hours, or 3 hours of accumulation time (Table 6).

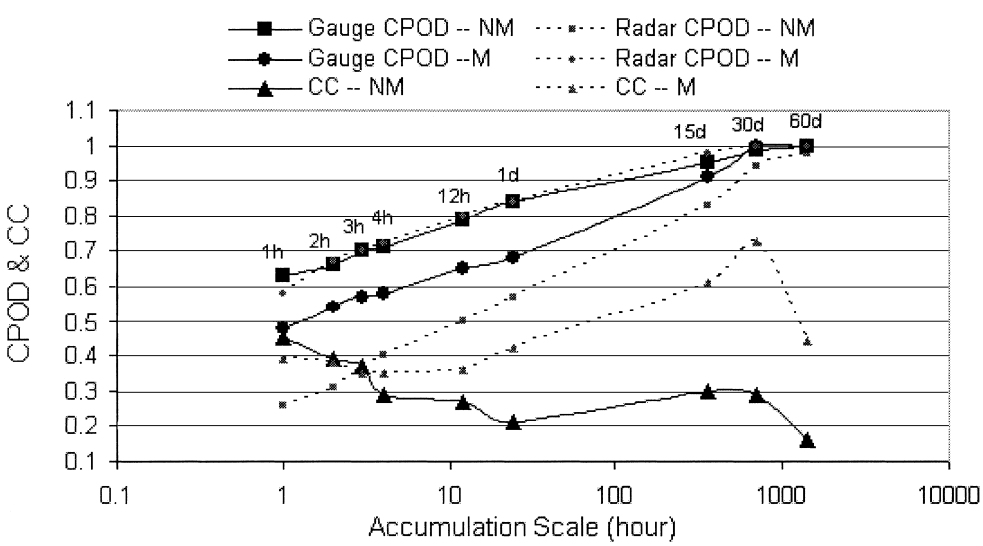

Figure 11. Conditional Probability of Rainfall Detection (CPOD) CPOD (Equations (2 and3) and Correlation Coefficient (CC) (Equation 4) of the Radar and Gauge Estimates on Different Accumulation Temporal Scales.

TABLE 6. Conditional Mean (CM) of Concurrent Gauge and Radar Estimates (1998 to 2001) at Various Temporal Scales.

Temporal Scale	NM – CM (mm)		M – CM (mm)		Sample Size	
	Radar	Gauge	Radar	Gauge	NM	M
1h	2.00	1.77	3.27	2.67	468	973
2h	2.35	2.23	3.92	3.20	430	882
3h	2.52	2.66	4.68	3.57	418	813
4h	2.68	3.02	4.96	3.76	395	781
12h	3.12	4.13	6.84	4.67	356	657
1d	3.57	4.95	7.68	5.24	326	601
15d	6.60	9.82	32.38	19.62	190	163
30d	9.72	14.60	53.92	32.32	134	99
60d	15.90	24.62	106.76	63.98	82	53
Event	3.21	4.25	6.21	4.60	308	640

Notes: NM: Nonmonsoon season (October to May).
M: Monsoon season (June to September).

DISCUSSION

Implications From Maximum Hourly Rainfall Rates

By examining the maximum hourly precipitation in the monsoon seasons of 1995 to 2001 (Figure 8), the gauge estimates are in the range of 25.13 to 50.85 mm/h, while the radar estimates are within 25.85 to 39.81 mm/h. The maximum radar estimate (39.81 mm/h) was less than the maximum gauge estimate (50.85 mm/h). The maximum gauge estimate of 50.85 mm/h was collected ending at 14:00 MST on July 4, 1998, by Gauge 42 (the highest site in the Sevilleta NWR, see Figure 2 and Table 1), located on the east slope of the Los Pinos Mountains, while the corresponding collocated radar cell estimation was only 9.03 mm/h. The maximum radar estimate of 39.81 mm/h was observed ending at 16:00 MST on August 27, 1999, while the corresponding collocated Gauge 42 collected 24.46 mm/h, smaller than the radar estimate. The differences of the maximum radar and gauge estimates are identified as point and area measurement errors since (1) the larger spatial variability of rainstorms could result in small or no rainfall measurement at the gauge site, while the radar has a higher probability of observing light to heavy rainfalls if they are within the collocated cell leading to higher rainfall measurement by the radar than by the gauge; and (2) a large rainfall rate observed by the gauge may not represent the areal average of rainfall within a radar cell, resulting in a difference between the gauge and radar observations. These mismatches could indicate extreme rainfall events or the spatial inhomogeneity of convective isolated thunderstorms.

Truncation and CPOD

Theoretically, the radar CPOD should be higher than the gauge CPOD since radar can "see" any rainfall event within a much larger area than a gauge (McCollum *et al.,* 2002). However, McCollum *et al.* (2002) found that P_{rg} is less than P_{gr} in the cold seasons from the 24-hour accumulation of NEXRAD HDP and gauge estimates. They listed two reasons for this: the radar beam overshooting in stratiform rainfall during cold seasons; and a truncation error caused by a computer source code problem in the NEXRAD rainfall processing at the NWS, especially during the lighter and long lasting rainfall (stratiform) in late winter to early spring (McCollum *et al.,* 2002; Seo *et al.*, 2000; Fulton *et al.,* 2003).

Figures 9 and 11, show the same observation for Stage III products: P_{rg} is less than P_{gr} in the nonmonsoon season (corresponding to the cold seasons). Three possible causes were considered that could contribute to the observed results: radar beam overshooting, capability of snowfall derivation, and truncation error. As discussed earlier (the Radar Data section), the radar beam overshooting of the Stage III data in the study area might result in uncertainty of rainfall estimates (under/overestimates) but not the total rainfall hours. This means that the beam overshooting in the study area does not result in the difference in radar or gauge CPOD.

There is no direct way to examine capability of snowfall detection using radar and rain gauge. One method for partitioning the precipitation into rain or snow is based on air temperature (Wigmosta *et al.,* 1994). Typically, precipitation is classified as snowfall when the air temperature is less than -1.1ºC and as rainfall when the air temperature is greater than 3.3ºC, or as a mixture when the air temperature is between -1.1ºC and 3.3ºC. In the study area, the snowfall events are very rare – usually about once or twice per year. Using these rules, it is found that there are 158 snowfall hours (air temperature less than -1.1ºC) from the total 4,181 hours of gauge precipitation (seven weather stations) in the nonmonsoon seasons during 1995 to 2001. This equals to 3.2 snowfall hours per gauge per year on average, which is very reasonable. In principle, the radar can detect snowfalls (Doviak and Zrnic, 1993), but the operational algorithms in the NWS do not yet calculate the snowwater equivalent (Mark A. Fresch, NWS, personal communication, May 21, 2004). Instead, these 158 snowfall hours are excluded from the radar precipitation products. For the air temperature ranging from -1.1ºC to 3.3ºC, there are 1,364 hours of mixed rainfall and snowfall events recorded by gauges. Within these 1,364 hours, Stage III only recorded 87 precipitation hours. This means that the other 1,277 hours of mixed snowfall and rainfall are missed or ignored in the radar product.

The third possible cause for P_{rg} being less than P_{gr} in the nonmonsoon season is the truncation error during light stratiform rainfall. Due to the CPU and RAM limitations in the "legacy" Radar Product Generator (RPG), the Precipitation Processing Subsystem (PPS) uses I*2 arithmetic rather than I*4 (NWS, 2002). Inconsistencies were found in the arithmetic that resulted in truncation, as opposed to rounding-off, of rainfall amounts, especially for long lasting small stratiform events (NWS, 2002). The truncation diminishes the rainfall rate by 1.5 to 2.0 mm/h for each hour when the rain continues steadily (McCollum *et al.,* 2002). Besides the radar PPS caused truncation problem, the radar recording mechanism and its sensitivity to small rainfall rates can also contribute to the truncation of rainfall hours. For example, on the one hand, the minimum hourly rainfall rate for the Stage III product is 0.01 mm/h. If a long lasting stratiform rainfall is 0.009 mm/h or intermittent rainfalls have an average rate of 0.009 mm/h, the hourly radar measurement is zero. On the other hand, the minimum hourly rainfall rate for a gauge is 0.1 mm/h. At first glance, the hourly measurement by the gauge is also zero. However, rain in the gauge is accumulated. After 12 hours (with a 0.009 mm/h rainfall), the gauge will have one hour of rainfall, but the radar still has none. Evaporation within the gauge may alleviate the problem, but during long lasting or cloudy days with intermittent rainfall, evaporation is often negligible, especially in winter. The first and most significant improvement for fixing the truncation errors, especially those due to the PPS itself, was not yet implemented in the data production across the United States until April to July 2002. The second and enhanced improvement was implemented in April to July 2003. The last improvement was planned to be implemented by the end of 2003 (Fulton *et al.,* 2003). Fulton *et al.'s* (2003) study showed a 250 percent larger rain area or a 148 percent larger maximum hourly rainfall rate than the corresponding nonfixed hourly digital precipitation array (DPA, corresponding to Stage I) for stratiform rainfalls, and a 120 percent larger rain area or a 15 percent larger maximum hourly rainfall rate for convective rainfalls, implying that the truncation error is more serious in the nonmonsoon season. However, as suggested by Fulton *et al.* (2003), the truncation impact on Stage III rainfall is not likely so large because the Stage III rainfall product has been calibrated by real-time gauge data. The data of 1995 to 2001 used for this study are Stage III and are prior to the first truncation fixing algorithm deployed in 2002. In the present study, the radar conditional mean precipitation in the nonmonsoon season is 1.60 mm/h, slightly larger than 1.03 mm/h of rain gauges (Table 5). It seems that there is no truncation error in terms of the conditional mean precipitation. However, in this study, the radar rainfall hours in the nonmonsoon seasons are much fewer than the gauge rainfall hours (see discussion below).

In general, it can be assumed that a collocated radar and gauge pair will detect the same precipitation event, maybe different precipitation amounts, at any given time. In particular for the nonmonsoon season, the rainfall variation is not significant within a radar cell. By roughly evaluating the rainfall hour truncation error, which is defined as the shortage of the rainfall hours as observed by the radar when compared with the ones as recorded by the gauge, the total rainfall hours recorded by the gauge are used as the reference rainfall hours. McCollum *et al.* (2002) attributed the truncation error of the lighter rainfall events in colder seasons to the lower radar detection probabilities (i.e., lower radar rainfall hours recorded by the radar than the rainfall hours recorded by the gauge). In the present study, however, the total hours (1,143) of radar precipitation observed during nonmonsoon seasons (1995 to 2001) are much fewer than those (4,181) from the gauge network (Table 5). Considering that the radar does not include the 158 snowfall events that should be removed from the gauge hours, the remaining hours from the gauges are still 252 percent larger than those from the radar. This means a 72 percent rainfall hour truncation by radar. If all 1,277 hours of the mixed rainfall and snowfall are treated as snowfall, which could be reasonable considering the high possibility that an ice particle can melt during the falling process while the radar measurement is taken when it is still in solid phase at higher altitude, the minimum truncation error by radar is still about 57 percent. This result suggests that (1) the loss of small rainfall events in the radar data caused by the rainfall hour truncation error is still serious (please note: discarding snowfall events discussed above is defined also as truncation cases); and (2) the truncation error caused loss of small rainfall events is not fixed by the real time rain gauge calibration as expected by Fulton *et al.* (2003). The gauge based bias adjustment may adjust the rainfall rates but cannot recover the lost rainfall hours of small rainfall events. This rainfall hour truncation error is an indirect indicator of truncation error in the rainfall amounts, which may contribute to a larger portion of NEXRAD underestimation for the nonmonsoonal precipitation accumulation because many of the rainfall events in the nonmonsoon season are just small precipitation rate events. Therefore, the truncation error of small rainfall hours may still be a major error source for both the much lower radar CPOD as compared to the gauge CPOD (Figures 9 and 11) and the radar underestimation of rainfall accumulation in the nonmonsoon season.

In the monsoon seasons, however, the situation is the opposite. Not only does the radar have larger conditional mean and rainfall accumulations than the gauge (Table 5), but also the total hours (3,900) of precipitation from the radar are larger than those (3,540) from the gauges (Table 4). Many factors could explain the radar gauge differences (radar overestimates in this case) in the monsoon season such as area point sampling error, radar hail contamination, radar Z-R relation error, radar bright band contamination, range dependence, virga, advection, and mosaicking of several radars (Austin, 1987; Pereira Fo *et al.,* 1998). The combination of all these factors could result in overestimates of radar rainfall. Truncation errors in monsoon seasons may be suppressed for two reasons: (1) the rainfall rate itself is much higher in the monsoon seasons than nonmonsoon seasons, thus the possibility that the rainfall rate over the truncation threshold is much higher; (2) the truncation error is overwhelmed by the combined effect of the factors mentioned above. This may explain why the radar underestimate is seldom observed in monsoon seasons. On the other hand, the radar overestimate resulting from meteorological phenomena such as hail contamination, virga, and advection more associated with monsoon seasons may overplay the underestimate due to truncation errors during the monsoon seasons.

Issues of Overestimation and Underestimation

In the concurrent 606 pairs of radar and gauge hourly precipitation during the nonmonsoon seasons of 1995 to 2001 (Table 5), there are 256 pairs of data with the radar estimates larger than the gauge estimates and vice versa for the other 350 pairs. In the 606 pairs, however, the radar rainfall CM (1.84 mm/h) is still larger than the gauge rainfall CM (1.74 mm/h) by 6 percent. Moreover, the radar rainfall CM (1.60 mm/h) on the total 1,143 hours is also larger than the gauge rainfall CM (1.03 mm/h) on the total 4,181 hours by 55 percent. Yet, the radar started to underestimate rainfall in the nonmonsoon season from the three-hour temporal scale onwards (Table 6) because of fewer hours of hourly radar precipitation measurements being added due to the rainfall hour truncation.

During the monsoon seasons, of the 1,331 pairs of radar and gauge hourly precipitation, there are 703 pairs with radar estimates larger than the gauges and vice versa for the other 628 pairs. It is clear that the radar CM (3.07 mm/h) of the 1,331 pairs is larger than the gauge CM (2.72 mm/h) of the 1,331 pairs by 13 percent. The radar CM (2.65 mm/h) on 3,900 hours is also larger than the gauge CM (2.00 mm/h) on 3,540 hours by 33 percent. A higher CM, combined with slightly more hours recorded, produces larger rainfall accumulation estimates in the monsoon seasons by radar.

As for the seasonal precipitation accumulation, radar underestimates it by 18 to 89 percent in the nonmonsoon seasons, and overestimates it by 11 to 88 percent in the monsoon seasons. These results are different from those of Young *et al.* (2000), Fortune (2002), Pereira Fo *et al.* (1998), and Jayakrishnan *et al.* (2004). Their results show consistent radar (Stage III) underestimation in the central and eastern United States.

From the CM precipitation point of view, the radar CMs of the radar gauge pairs (1.84 mm/h and 3.07 mm/h for nonmonsoon and monsoon seasons, respectively) are larger than the radar CMs of the total count (1.60 mm/h and 2.65 mm/h). The gauge CMs of radar gauge pairs (1.74 mm/h and 2.72 mm/h) are also larger than the gauge CMs of the total count (1.03 mm/h and 2.00 mm/h). These observations indicate that the chance for both the radar and the gauge to detect a rainfall event concurrently is larger when the rainfall itself is heavier.

From the standpoint of seasonal accumulation, radar overestimates rainfall in the monsoon seasons and underestimates it in the nonmonsoon seasons when compared with the gauges. However, considering that radar is more capable of producing better areal precipitation estimates in the monsoon season, it may suggest that NEXRAD Stage III estimation could be a better rainfall product in terms of areal average rainfall than the estimation from sparse gauge networks in the monsoon season. This matches the general practice at Arkansas-Red Basin RFC: NEXRAD Stage III works well in warmer seasons (Seo and Breidenbach, 2002; NWS, 2002).

SUMMARY AND CONCLUSIONS

This study conducted a comparison between the NEXRAD Stage III and rain gauge precipitation estimations during the time period of 1995 to 2001 in the Sevilleta National Wildlife Refuge. The NEXRAD Stage III was evaluated using gauge data as the reference. The results from the analysis of the probability distribution of radar and gauge rainfall rates indicate that the lower rainfall rates account for a large portion of the total rainfall hours, but only a small portion of the total rainfall accumulation. Gauges record a large percentage of rainfall hours and rainfall accumulation at small rain rates as compared with the radar product. The Stage III radar data records a large percentage of rainfall hours and rainfall accumulation at large rain rates as compared with the rain gauges.

Statistical analyses suggest that the radar overestimates hourly CM precipitation in all seasons, underestimates rainfall accumulation in the nonmonsoon season, and overestimates rainfall accumulation in the monsoon season. Average CM, maximum precipitation, and conditional variance of precipitation have the same seasonal patterns: larger radar estimates in the monsoon seasons and lower radar estimates in the nonmonsoon seasons as compared with those from gauges. In general, the point gauge estimation is more scattered than the areal radar estimation.

The CPOD from both radar and gauge increases as the temporal scale increases. The CC of rainfall amounts between radar gauge data pairs increases to a maximum of 0.73 at the 30-day temporal scale during the monsoon season, while the largest value of CC (0.48) in the nonmonsoon season is at the 1-hour temporal scale.

Results from both the precipitation hours and CPOD confirm that the truncation error may still be a major error source in the NEXRAD Stage III data for the non-monsoon seasons, while overestimates associated with area point sampling error, hail contamination, virga, advection, etc., may be the major error sources in the NEXRAD Stage III data during the monsoon seasons. These overestimates may suppress the truncation error caused underestimates in the monsoon seasons. It seems that the real time gauge calibration to the Stage II and Stage III products has not effectively corrected the truncation errors for the nonmonsoon season as discussed by Fulton *et al.* (2003). The major difference in rainfall estimates between radar and gauge in the monsoon seasons may be mainly due to area point sampling error, radar Z-R relation error, radar hail contamination, radar bright band contamination, radar range dependence, virga, advection, and mosaicking of several radars. More caution is suggested in using Stage III data for nonmonsoonal (stratiform) rainfall events (prior to the truncation fixed algorithm deployed in 2002), as the truncation error can be a significant drawback.

ACKNOWLEDGMENTS

This work was supported by the NSF EPSCoR grant EPS-0132632 through the Institute of Natural Resources Analysis and Management in New Mexico. The authors acknowledge and appreciate Sevilleta Long-Term Ecological Research Program (LTER) at the University of New Mexico for sharing GIS resources and weather data. The authors thank Dr. Brian Nelson at the National Climate Data Center for his thoughtful comments to the manuscript. The authors also thank Doug Moore at the Sevilleta LTER for providing detailed information on the rain gauges and Dr. Brian Borchers and Susan Delap (New Mexico Tech) for reviewing and editing the manuscript. The authors would like to thank three anonymous reviewers for their very helpful comments, suggestions, and corrections that substantially improved this paper.

LITERATURE CITED

Anagnostou, E.N, W.F. Krajewski, and J. Smith, 1999. Uncertainty Quantification of Mean-Areal Radar-Rainfall Estimates. Journal of Atmospheric and Oceanic Technology 16:206-215.

Austin, P.M., 1987. Relation Between Measured Radar Reflectivity and Surface Rainfall. Monthly Weather Review 115:1053-1070.

Bedient, P.B, B.C. Hoblit, D.C. Gladwell, and B.E. Vieux, 2000. NEXRAD Radar for Flood Prediction in Houston. Journal of Hydrologic Engineering 5:269-277.

Bradley, A.A., C. Peters-Lidard, B.R. Nelson, J.A. Smith, and C.B. Yong, 2002. Raingauge Network Design Using NEXRAD Precipitation Estimates. Journal of the American Water Resources Association (JAWRA) 38:1393-1407.

Ciach, G.J. and W.F. Krajewski, 1999. Radar-Rain Gauge Comparisons Under Observational Uncertainties. Journal of Applied Meteorology 38:1519-1525.

Dahm, C.N. and D.L. Moore, 1994. The El Niño/Southern Oscillation Phenomenon and the Sevilleta Long-Term Ecological Research Site. *In:* LTER Report: LTER Climate Committee, D. Greenland (Editor). LTER Publication No. 18, University of Washington, Seattle, Washington, pp. 12-20.

Doviak, R.J. and D.S. Zrnic, 1993. Doppler Radar and Weather Observations (Second Edition). Academic Press, San Diego, California, 562 pp.

Finnerty, B.D., M.B. Smith, D.-J. Seo, V. Koren, and G.E. Moglen, 1997. Space-Time Scale Sensitivity of the Sacramento Model to Radar-Gage Precipitation Inputs. Journal of Hydrology 203:21-38.

Fortune, M.A., 2002. Verification of Precipitation Fields From Multiple Sources (including Satellite) in the New RFC-Wide Precipitation Processing System. *In:* Preprints, Interactive Symposium on the Advanced Weather Interactive Processing System (AWIPS), Orlando, Florida. American Meteorological Society, Boston, Massachusetts, J168-169.

Fulton, R.A., J.P Breidenbach, D.J. Seo, and D.A. Miller, 1998. The WSR-88D Rainfall Algorithm. Weather and Forecasting 13:377-395.

Fulton, R.A., F. Ding, and D.A. Miller, 2003. Truncation Errors in Historical WSR-88D Rainfall Products. *In:* Proceedings of 31st Conference on Radar Meteorology, Seattle, Washington. American Meteorological Society, Boston, Massachusetts, CD-ROM.

Grassotti, C., R.N. Hoffman, E.R. Vivoni, and D. Entekhabi, 2003. Multiple Timescale Intercomparison of Two Radar Products and Rain Gauge Observations Over the Arkansas-Red River Basin. Weather and Forecasting 18(6):1207-1229.

Habib, E. and W.F. Krajewski, 2002. Uncertainty Analysis of the TRMM Ground-Validation Radar-Rainfall Products: Application to the TEFLUN-B Field Campaign. Journal of Applied Meteorology 41:558-572.

Habib, E., W.F. Krajewski, and A. Kruger, 2001. Sampling Errors of Tipping-Bucket Rain Gauge Measurements. Journal of Hydrologic Engineering 6:159-166.

Hobbie, J.E., S.R. Carpenter, N.B. Grimm, J.R. Gosz, and T.R. Seastedt, 2003. The US Long Term Ecological Research Program. BioScience 53:21-32.

Jayakrishnan, R., R. Srinivasan, and J.G. Arnold, 2004. Comparison of Raingage and WSR-88D Stage III Precipitation Data Over the Texas-Gulf Basin. Journal of Hydrology, 292: 135-152

Johnson, D., M. Smith, V. Koren, and B. Finnerty, 1999. Comparing Mean Areal Precipitation Estimates From NEXRAD and Rain Gauge Networks. Journal of Hydrologic Engineering 4(2):117-124.

Kitchen, M. and R.M. Blackall, 1992. Representativeness Errors in Comparisons Between Radar and Gauge Measurements of Rainfall. Journal of Hydrology 134:13-33.

Krajewski, W.F., 1987. Co-Kriging of Radar-Rainfall and Rain Gauge Data. Journal of Geophysical Research 92:9571-9580.

Krajewski, W.F., G.J. Ciach, and E. Habib, 2003. An Analysis of Small-Scale Rainfall Variability in Different Climate Regimes. Hydrologic Sciences Journal 48:151-162.

Krajewski, W.F. and J.A. Smith, 2002. Radar Hydrology: Rainfall Estimation. Advances in Water Resources 25:1387-1394.

Maddox, R.A., J. Zhang, J.J. Gourley, and K.W. Howard, 2002. Weather Radar Coverage Over the Contiguous United States. Weather Forecasting 17:927-934.

McCollum, J.R., W.E. Krajewski, and R.R. Ferraro, 2002. Evaluation of Biases of Satellite Rainfall Estimation Algorithms Over the Continental United States. Journal of Applied Meteorology 41:1065-1080.

Moore, D., 1996. A Climatic Analysis of Long-Term Ecological Research Sites: Chapter 17, Sevilleta National Wildlife Refuge. *Available at* http://intranet.lternet.edu/archives/documents/Publications/climdes/sev/sevclim.htm. Accessed in September 2003.

Morin, W., W.E. Krajewski, D.C. Goodrich, X. Gao, and S. Sorooshian, 2003. Estimating Rainfall Intensities From Weather Radar Data: The Scale-Dependency Problem. Journal of Hydrometeorology 4:782-797.

NGDC (National Geophysical Data Center), 2003. The Global Land One-km Base Elevation (GLOBE) Project. *Available at* http://www.ngdc.noaa.gov/mgg/topo/globe.html. *Accessed in* February 2003.

NWS (National Weather Service), 2002. Distributed Model Intercomparison Project: About the Stage III Data. *Available at* http://www.nws.noaa.gov/oh/hrl/dmip/stageiii_info.htm. *Accessed in* October 2003

NWS (National Weather Service), 2003. WGRFC Operational NEXRAD Stage III Data. Hydrologic Data Systems Branch. *Available at* http://dipper.nws.noaa.gov/hdsb/data/nexrad/wgrfc_stageiii.php. *Accessed in* May 2003.

Ormsby, T., E. Napoleon, R. Burke, C. Groessl, and L. Feaster, 2001. Getting to Know ArcGIS Desktop. Environmental Systems Research Institute, Inc., Redlands, California, 588 pp.

Pereira Fo, A.J. and K.C. Crawford, 1999a. Mesoscale Precipitation Fields. Part I: Statistical Analysis and Hydrologic Response. Journal of Applied Meteorology 38:82-101.

Pereira Fo, A.J., K.C. Crawford, and C.L. Hartzell, 1998. Improving WSR-88D Hourly Rainfall Estimates. Weather and Forecasting 13:1016-1028.

Pereira Fo, A.J., K.C. Crawford, and D.J. Stensrud, 1999b. Mesoscale Precipitation Fields. Part II: Hydrometeorologic Modeling. Journal of Applied Meteorology 38:102-125.

Reed, S.M. and D.R. Maidment, 1995. A GIS Procedure for Merging NEXRAD Precipitation Data and Digital Elevation Models to Determine Rainfall-Runoff Modeling Parameters. CRWR Online Report 95-3. *Available at* http:www.ce.utexas.edu/prof/maidment/gishyd97/library/nexrad/rep95_3.htm.

Reed, S.M. and D.R. Maidment, 1999. Coordinate Transformations for Using NEXRAD Data in GIS-Based Hydrologic Modeling. Journal of Hydrologic Engineering 4:174-182.

Seo, D.J. and J.P. Breidenbach, 2002. Real-Time Correction of Spatially Nonuniform Bias in Radar Rainfall Data Using Rain Gauge Measurements. Journal of Hydrometeorology 3:93-111.

Seo, Dong-Jun, Jay Breidenbach, Richard Fulton, Dennis Miller, Bertrand Vignal, and Witold Krajewski, 2000. Final Report for June 1, 1999 to May 31, 2000: Interagency Memorandum of Understanding Among the NEXRAD Program, The WSR-88D Operational Support Facility, and The National Weather Service Office of Hydrology. National Weather Service, Hydrology Lab. *Available at* http://www.nws.noaa.gov/oh/hrl/papers/2000mou/Report/Index.html. *Accessed in* October 2003.

Shah, S.M.S., P.E. O'Conell, and J.R.M. Hosking, 1996. Modeling the Effects of Spatial Variability in Rainfall on Catchment Response. 2. Experiments With Distributed and Lumped Models. Journal of Hydrology 175:9-111.

Short, D.A. and K. Nakamura, 2000. TRMM Radar Observations of Shallow Precipitation Over the Tropical Oceans. Journal of Climate 13:4107-4124.

Smith, J.A., M.L. Baeck, J.E. Morrison, and P. Sturdevant-Rees, 2002. The Regional Hydrology of Extreme Floods in an Urbanizing Drainage Basin. Journal of Hydrometeorology 3:267-282.

Smith, J.A., M.L. Baeck, Y. Zhang, and C.A. Doswell, 2001. Extreme Rainfall and Flooding From Supercell Thunderstorms. Journal of Hydrometeorology 2:469-489.

Smith, J.A., D.J. Seo, M.L. Baeck, and M.D. Hudlow, 1996. An Intercomparison Study of NEXRAD Precipitation Estimates. Water Resources Research 32:2035-2045.

Stellman, K.M., H.E. Fuelberg, R. Garza, and M. Mullusky, 2000. An Examination of Radar- and Rain Gauge-Derived Mean Areal Precipitation over Georgia Watersheds. Weather and Forecasting 16(1):133-144.

University of New Mexico, 2003. Sevilleta LTER Research: Research: Local: Climate: Meteorology: Overview. *Available at* http://sevilleta.unm.edu/research/local/climate/meteorology/overview/. *Accessed in* January 2003.

Vieux, B.E. and P.B. Bedient, 1998. Estimation of Rainfall for Flood Prediction From WSR-88D Reflectivity: A Case Study. Weather and Forecasting 13(2):407-415.

Wang, D., M.B. Smith, Z. Zhang, S. Reed, and V. Koren, 2000. Statistical Comparison of Mean Areal Precipitation Estimates From WSR-88D, Operational and Historical Gauge Networks. *In:* Preprints, 15th Conference on Hydrology, Long Beach, California. American Meteorological Society, Boston, Massachusetts, pp. 107-110.

Wigmosta, M.S., L.W. Vail, and D.P. Lettenmaier, 1994. A Distributed Hydrology-Vegetation Model for Complex Terrain. Water Resources Research 30:1665-1679.

Winchell, M., H.V. Gupta, and S. Sorooshian, 1998. On the Simulation of Infiltration and Saturation-Excess Runoff Using Radar-Based Rainfall Estimates: Effects of Algorithm Uncertainty and Pixel Aggregation. Water Resources Research 34:2655-2670.

Xie, H., E.E. Small, J.M.H. Hendrickx, M. Richmond, and X. Zhou, 2003. GIS Based NEXRAD Precipitation (Stage III) Database. *In:* Proceedings of the ESRI 2003 User Conference, San Diego, California, 16 pp. Environmental Systems Research Institute, Inc., Redlands, California, CD-ROM.

Xie, H., X. Zhou, E.R. Vivoni, J.M.H. Hendrickx, E.E. Small, 2005. GIS Based NEXRAD Precipitation Database: Automated Approaches for Data Processing and Visualization. Computers and Geosciences 31:65-76.

Young, C.B., B.R. Nelson, A.A. Bradley, W.F. Krajewski, A, Kruger, and M.L. Morrissey, 2000. Evaluating NEXRAD Multisensor Precipitation Estimates for Operational Hydrologic Forecasting. Journal of Hydrometeorology 1:241-254.

Young, C.B., B.R. Nelson, A.A. Bradley, J.A. Smith, C.D. Peters-Lidard, A. Kruger, and M.L. Baeck, 1999. An Evaluation of NEXRAD Precipitation Estimates in Complex Terrain. Journal of Geophysical Research 104(D16):19691-19703.
Zawadzki, I., 1975. On Radar-Raingauge Comparison. Journal of Applied Meteorology 14:1430-1436.
Zhang, Y. and J.A. Smith, 2003. Space-Time Variability of Rainfall and Extreme Flood Response in the Menomonee River Basin, Wisconsin. Journal of Hydrometeorology 4:506-517.